

Homepage: <http://jusami.batan.go.id>

Jurnal Sains Materi Indonesia

Akreditasi No : 21/E/KPT/2018

Date 9 July 2018

ISSN 1411-1098

E-ISSN 2614-087X

## SYNTHESIS AND CHARACTERIZATION OF $\text{Li}_4\text{Ti}_5\text{O}_{12}$ WITH SOL GEL METHOD AS A LITHIUM-ION BATTERY ANODE MATERIAL

Slamet Priyono<sup>1</sup>, Ilma Nuroniah<sup>2</sup>, Achmad Subhan<sup>1</sup>, Edi Sanjaya<sup>2</sup>, Bambang Prihandoko<sup>1</sup>

<sup>1</sup>Research Center for Physics – Indonesian Institute of Science, Tangerang Selatan, Indonesia

<sup>2</sup>Physics Departemen, UIN Syarif Hidayatullah, Jakarta, Indonesia

E-mail: [slam013@lipi.go.id](mailto:slam013@lipi.go.id)

Received: 12 September 2018

Revised: 30 November 2018

Accepted: 6 December 2018

### ABSTRACT

**SYNTHESIS AND CHARACTERIZATION OF  $\text{Li}_4\text{Ti}_5\text{O}_{12}$  WITH SOL GEL METHOD AS A LITHIUM ION-BATTERY ANODE MATERIAL.** Synthesis of anode  $\text{Li}_4\text{Ti}_5\text{O}_{12}$  material has been carried out using the sol gel method. The synthesis is carried out with variations in sintering temperatures at 500 °C, 600 °C, 700 °C dan 800 °C. Characterization carried out includes testing thermal analysis to determine the optimum temperature for sintering, XRD (X-ray Diffraction) to find out the phase formation of  $\text{Li}_4\text{Ti}_5\text{O}_{12}$ , Scanning electron microscope (SEM) to analyse the morphology formed, testing Cyclic voltammetry, charge-discharge and Electrochemical Impedance Spectroscopy (EIS) is carried out to find out the electrochemical performance. From the results of characterization of thermal and XRD analyses, the optimum temperature for synthesis is 800°C with small impurity content. The results of SEM characterization show that the morphology of the sample is not homogeneous, and the particles are agglomerated. The resulting electrochemical performance increases along with the increase in temperature for sintering, including voltammogram graphs, diffusion coefficient values, electrical conductivity and charge-discharge capacity. Of all the samples, the LTO sintered at 800°C shows good electrochemical performance with a sharp and good voltammogram graph, diffusion coefficient value of lithium ion is  $1.58 \times 10^{-9} \text{ cm}^2\text{s}^{-1}$ , electrical conductivity of 0.6282 S/cm and the discharge capacity given is 78,07 mAh/g.

**Keywords:**  $\text{Li}_4\text{Ti}_5\text{O}_{12}$  anode, Sol gel method, Lithium Ion Battery.

### ABSTRAK

**SINTESIS DAN KARAKTERISASI  $\text{Li}_4\text{Ti}_5\text{O}_{12}$  DENGAN METODE SOL GEL SEBAGAI MATERIAL ANODA BATERAI ION LITHIUM.** Telah dilakukan sintesis material anoda  $\text{Li}_4\text{Ti}_5\text{O}_{12}$  dengan menggunakan metode sol gel. Sintesis dilakukan dengan variasi suhu sintering pada suhu 500°C, 600°C, 700°C dan 800°C. Karakterisasi yang dilakukan meliputi pengujian analisa termal untuk menentukan suhu optimum untuk sintering, XRD (X-ray Diffraction) untuk mengetahui pembentukan fasa  $\text{Li}_4\text{Ti}_5\text{O}_{12}$ , Scanning electron microscope (SEM) untuk menganalisa morfologi yang terbentuk, untuk mengetahui performa elektrokimia dilakukan pengujian *Cyclic voltammetry*, *charge-discharge* dan *Electrochemical Impedance Spectroscopy* (EIS). Dari hasil karakterisasi analisa termal dan XRD, suhu optimum untuk sintesis yaitu pada suhu 800°C dengan kandungan impuritas yang kecil. Hasil karakterisasi SEM menunjukkan morfologi sampel tidak homogen, partikel beragglomerasi. Performa elektrokimia yang dihasilkan mengalami peningkatan seiring dengan naiknya suhu sinter, meliputi grafik voltammogram, nilai koefisien difusi, konduktivitas listrik dan kapasitas charge-discharge. Dari semua sampel, LTO yang disinter pada suhu 800°C menunjukkan performa elektrokimia yang baik dengan grafik voltammogram yang tajam dan bagus, nilai koefisien difusi ion lithium sebesar  $1,58 \times 10^{-9} \text{ cm}^2\text{s}^{-1}$ , konduktivitas listrik sebesar 0.6282 S/cm dan kapasitas *discharge* yang diberikan sebesar 78,07 mAh/g.

**Kata kunci:** Anoda  $\text{Li}_4\text{Ti}_5\text{O}_{12}$ , Metode Sol gel, Baterai Ion Lithium

### INTRODUCTION

Along with the development of technology, the necessity for electricity storage is increasing. Almost all modern technologies such as portable equipment (cellphones, laptops, digital cameras, etc.), medical implant applications such as artificial hearts, electric bicycles, HEV (Hybrid Electric Vehicles) electric

cars, wind or solar power storage which have now been developed by a number of researchers need an electrical energy storage that can support these technological needs [1]. One form of electrical energy storage is a battery. Secondary batteries or commonly known as rechargeable Lithium-Ion Batteries (LIB) work based on

the intercalation ability of  $\text{Li}^+$  ions which move continuously between the anode and cathode during the charge-discharge process [2]. The research and development of lithium ion batteries began in 1980 at Asahi Chemical and began the commercialization in 1990 by Sony Corporation for Kyocera cellular phones and camcorders. Since then, the market growth for Li-ion batteries has reached \$4 billion in 2005. This happened as the advantages of lithium ion batteries, besides being rechargeable, this battery has a high energy density, light in weight, no memory effect, a good life cycle, high energy efficiency and good high-rate capability leads to many uses of this battery in various applications [3].

The anode active material which is currently widely used is graphite while for cathode material is lithium cobalt oxide ( $\text{LiCoO}_2$ ) [2]. Graphite as an anode material has a very large specific energy storage capacity of 372 mAh/g (850 mAh/cm<sup>3</sup>) in theoretical calculations [3-6]. Although this material has a large storage capacity, it also has a weakness in its safety, including an organic decomposition of electrolytes and the formation of lithium ion dendrites on the surface of the graphite causing this material to be no longer safe to use. In addition, graphite anodes undergo lattice volume expansion (9-13%) during the intercalation process of  $\text{Li}^+$  ion which may result in the drastic reduction of storage capacity for several cycles during the charge-discharge process [5,7-9]. This weakness causes the graphite application to be limited to the next Li-ion battery, so re-placement materials are needed as alternative energy storage.

Lithium Titanium Oxide ( $\text{Li}_4\text{Ti}_5\text{O}_{12}$ ) is one of the promising candidates for substitute material for graphite anodes. With its characteristics as a "zero-strain insertion compound" material, this material has a strong spinel structure so that during the charge-discharge process, it does not result in changes in lattice volume. In addition,  $\text{Li}_4\text{Ti}_5\text{O}_{12}$  has a stable working voltage of 1.55V vs  $\text{Li}^+/\text{Li}$ , so there is no growth of lithium ion dendrites during the intercalation process [6-7, 10-11]. Of course, this shows that  $\text{Li}_4\text{Ti}_5\text{O}_{12}$  is safer than graphite to use as an anode material. As for the other advantages is a fairly high storage capacity of 175 mAh/g, not contain toxic materials, its availability is abundant and the price is relatively cheap [7,12]. However,  $\text{Li}_4\text{Ti}_5\text{O}_{12}$  shows low electronic conductivity (in the range  $10^{-8}$  to  $10^{-13}$  S cm<sup>-1</sup>) and a low diffusion coefficient of lithium ions of around  $10^{-8}$  to  $10^{-13}$  cm<sup>2</sup> s<sup>-1</sup>, causing this material to have the ability to condition high rate during the charge-discharge process which is also low [7,8,9]. There are several ways to improve this deficiency of  $\text{Li}_4\text{Ti}_5\text{O}_{12}$  by conducting a synthesis using new methods, doping with metal or non-metallic ions on Li, Ti or O sites, carbon coatings, and also by combining the three methods.

Previously, many studies have been conducted on the synthesis of  $\text{Li}_4\text{Ti}_5\text{O}_{12}$  using the solid state reaction method, this method is broadly used because the

process is easy and simple. Mixing is conducted mechanically, the mixture is less homogeneous, the morphology is irregular, the particle size is large, distribution of particle size is wide and stoichiometric control is low [6,8,9,13]. Therefore, another method is needed to synthesize  $\text{Li}_4\text{Ti}_5\text{O}_{12}$  material using a sol-gel method. This method can reduce the sintering temperature, cut down particle size, the mixture is more homogeneous, the morphology is more regular. Cutting down the particle size will reduce the diffusion path of  $\text{Li}^+$  atom so that the expected electronic conductivity value and the diffusion coefficient of the lithium ion will increase.

In this study, the synthesis and characterization of  $\text{Li}_4\text{Ti}_5\text{O}_{12}$  anode material using the sol-gel method will be carried out in order to determine the optimum temperature of  $\text{Li}_4\text{Ti}_5\text{O}_{12}$  phase formation, in addition to increasing electronic conductivity and diffusion coefficient of lithium ions. In general, making  $\text{Li}_4\text{Ti}_5\text{O}_{12}$  through the sol gel method uses LiOH with water solvents and TTIP with ethanol solvents, but differences in polar and non-polar solvents cause the mixture to be non-homogeneous. In this study, LiOH raw materials were dissolved in ethanol solvents which have not been widely studied. Although LiOH has a low solubility in ethanol, using the same solvent, a more homogeneous mixture will be obtained.

## EXPERIMENTAL METHOD

### Materials and Equipments

In this study, the making of  $\text{Li}_4\text{Ti}_5\text{O}_{12}$  anode material uses Pro Analysis raw materials including Lithium Hydroxide (LiOH) powder, Merck Germany; Titanium (IV) Isopropoxide or TTIP ( $\text{C}_{12}\text{H}_{28}\text{O}_4\text{Ti}$ ), Sigma Aldrich; Citric Acid ( $\text{C}_6\text{H}_8\text{O}_7$ ), Sigma Aldrich as a chelating agent, and ethanol ( $\text{C}_2\text{H}_5\text{OH}$ ), Merck Germany as a solvent. To make electrode sheets, additional materials were used in addition to  $\text{Li}_4\text{Ti}_5\text{O}_{12}$  active material, i.e. PVDF, super P and DMAC solvents. Whereas for coin cell making, the materials used include lithium metal,  $\text{LiPF}_6$  electrolytes, and a set of coin cell.

XRD (X-Ray Diffractometer) instrument, Rigaku with SmartLab 3 kW type was used to determine the phase composition and crystal structure of the powder of  $\text{Li}_4\text{Ti}_5\text{O}_{12}$  active material. In addition, to analyze the morphological structure of the material used, Scanning Electron Microscope (SEM) instrument, Hitachi SU3500 was used. WonAtech WBCS3000, Korean instrument, was used to conduct testing of Cyclic Voltammetry and Charge Discharge Capacity. LCR meter Hioki 353250 chemical impedance meter instrument was used for Electrochemical Impedance Spectroscopy (EIS) test.

### Procedure

$\text{Li}_4\text{Ti}_5\text{O}_{12}$  active material was synthesized using the sol gel method following a stoichiometric calculation. First, Lithium hydroxide (LiOH) was dissolved in ethanol so that A solution was formed, then

dissolved Titanium (IV) Isopropoxide ( $\text{C}_{12}\text{H}_{28}\text{O}_4\text{Ti}$ ) in ethanol, thus B solution was formed. After stirring for 1 hour, both solutions were mixed while stirring until the sol was formed. Citric acid was added to the solution and stirred for 3 hours until a gel was formed. The gel was dried at  $80^\circ\text{C}$  for 2 days, then sintered at temperatures of  $500^\circ\text{C}$ ,  $600^\circ\text{C}$ ,  $700^\circ\text{C}$  and  $800^\circ\text{C}$  for 2 hours.

In order to find out the electrochemical performance of the battery, an anode sheet was made by mixing active material ( $\text{Li}_4\text{Ti}_5\text{O}_{12}$ ) with PVDF (polyvinylidene fluoride) as a binder and super P as a conductive material with a composition ratio of 85:10:5 in DMAC solution. The formed mixture was coated on Cu foil placed on top of the Automatic Thick Film Coater. The samples were dried at  $60^\circ\text{C}$  and then stored in an oven at  $50^\circ\text{C}$ .

Battery cells made were coin cell type batteries which were arranged to form half cells. The anode sheet was cut in a circle with a diameter of 16 mm, metallic Li was used as a counter electrode and  $\text{LiPF}_6$  as an electrolyte. Everything was arranged in a glove box. Cyclic voltammetry testing was conducted by connecting cells with Battery Cycler, cell voltage as input, increased and decreased alternately at a range of 0.75-2.8 Volt with scan rate of 0.12 mV/s. Charge Discharge testing was conducted to determine the electrical capacity that cells could produce. Electrochemical Impedance Spectroscopy (EIS) testing was carried out at a frequency of 0.5 - 20 kHz.

## RESULTS AND DISCUSSION

The precursors produced using the sol gel method were then tested for Thermal Analysis to determine the sintering temperature and thermal characters. The thermal characterization results of the precursor  $\text{Li}_4\text{Ti}_5\text{O}_{12}$  with STA is shown in Figure 1. The reduction in mass in TG curve in Figure 1 occurs in 3 stages, namely at a temperature range of  $45^\circ\text{C}$  -  $241^\circ\text{C}$ ,  $241^\circ\text{C}$  -  $470^\circ\text{C}$  and  $470^\circ\text{C}$  -  $800^\circ\text{C}$ . The first reduction at a temperature range of  $45^\circ\text{C}$  -  $241^\circ\text{C}$  has a significant reduction in mass, namely 30.11%. In the first stage, the process of releasing  $\text{H}_2\text{O}$  water vapor,  $\text{CO}_2$  gas, volatile substances and ethanol as a solvent occur during the synthesis of  $\text{Li}_4\text{Ti}_5\text{O}_{12}$ . In addition, there is also a decomposition process of citric acid and titanium (IV) isopropoxide. Then the second reduction occurred at a mass reduction of 10.3%, this decrease was due to the decomposition process of titanium (IV) isopropoxide which still occurred (at a temperature range of  $241$ - $358^\circ\text{C}$ ) and decomposition of  $\text{LiOH}$  (at a temperature range of  $358^\circ\text{C}$  -  $470^\circ\text{C}$ ). The reduction in the mass in the section is also due to the combustion process of citric acid, which is the breakdown of organic materials into carbon due to the heating process above the material decomposition temperature [13]. The third reduction in mass is at a temperature range of  $470^\circ\text{C}$  -  $800^\circ\text{C}$ , the decrease in mass is not too large, which is around

6.9%. In this third peak, there is a crystallization process, the  $\text{Li}_4\text{Ti}_5\text{O}_{12}$  phase begins to form and volatile substances are released. In this reduction, the phase formed tends to be stable.

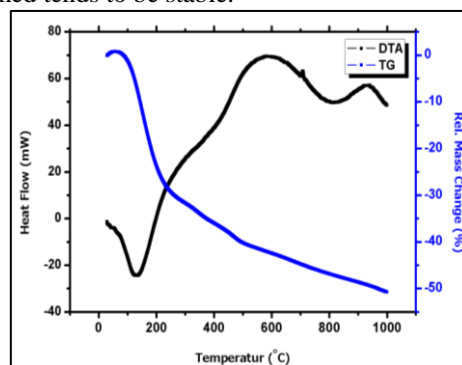


Figure 1. DTA/TG Graph of  $\text{Li}_4\text{Ti}_5\text{O}_{12}$

On the DTA curve, there is a peak with a downward curved shape at a temperature range of  $36^\circ\text{C}$  -  $240^\circ\text{C}$  with a maximum peak at a temperature of  $132^\circ\text{C}$ . This indicates an endothermic reaction, where this reaction occurs when the sample temperature is lower than the reference temperature. When the sample temperature is lower, the sample will absorb heat from the environment. In this temperature range, the material begins to be hydrated, dehydration becomes the first process in conducting a heating, in this process organic elements such as water vapor are released and the release of volatile substances such as  $\text{CO}_2$  gas. In addition, there is a decomposition process of citric acid, in the process of release until decomposition, energy (enthalpy) of  $706.69 \text{ J/g}$  is needed. Likewise at a temperature range of  $733^\circ\text{C}$  -  $969^\circ\text{C}$ , there is an endothermic peak with a maximum peak at a temperature of  $809^\circ\text{C}$ . This endothermic peak is the crystallization process of  $\text{Li}_4\text{Ti}_5\text{O}_{12}$  material, the  $\text{Li}_4\text{Ti}_5\text{O}_{12}$  phase has begun to form. The amount of energy needed for this crystallization process is  $293.8 \text{ J/g}$ .

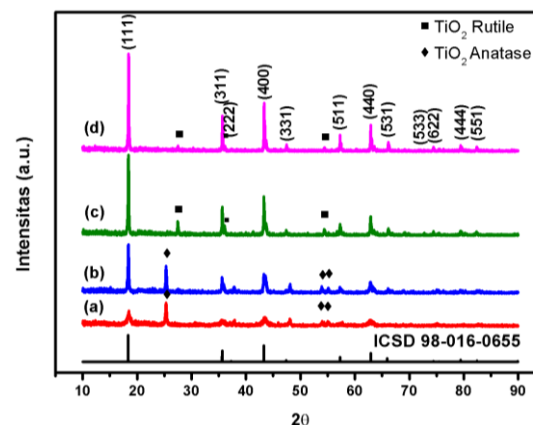


Figure 2. XRD curve of  $\text{Li}_4\text{Ti}_5\text{O}_{12}$  material with variations in sintering temperatures at (a)  $500^\circ\text{C}$ , (b)  $600^\circ\text{C}$ , (c)  $700^\circ\text{C}$  and (d)  $800^\circ\text{C}$  with a holding time of 2 hours.

Figure 2 is the XRD pattern of  $\text{Li}_4\text{Ti}_5\text{O}_{12}$  samples with sintering temperature variations, after matched with the database (ICSD-98-016-0655), there

is an intensity peak which indicates that the  $\text{Li}_4\text{Ti}_5\text{O}_{12}$  phase has been formed at a temperature range of 500 - 800°C with a cubic crystal structure and Fd3m space group, but there is still the impurity of  $\text{TiO}_2$  which does not react. However, along with the increase in temperature, the intensity peak which shows the  $\text{Li}_4\text{Ti}_5\text{O}_{12}$  phase is getting sharper while the peak which shows the impurity phase of  $\text{TiO}_2$  decreases. This increasingly narrow and sharp peak indicates that the size of the crystals formed from the  $\text{Li}_4\text{Ti}_5\text{O}_{12}$  phase is greater.

The analysis using HIGHSCORE PLUS software results in the magnitude of the composition of the phase formed between Lithium Titanate and  $\text{TiO}_2$  with variations in sintering temperatures for each sample which can be seen in table 1 as follows:

**Table 1.** Composition of  $\text{Li}_4\text{Ti}_5\text{O}_{12}$  phase and  $\text{TiO}_2$  with variations of sintering temperatures.

Name of samples	Phase of $\text{Li}_4\text{Ti}_5\text{O}_{12}$ (%)	Phase of $\text{TiO}_2$ (%)	Chi <sup>2</sup> ( $\chi^2$ )
500°C	60.3	39.7	1.2
600°C	66.2	33.8	1.3
700°C	83.5	16.5	1.3
800°C	93.7	6.3	1.2

From table 1, the percentage of phase composition of  $\text{Li}_4\text{Ti}_5\text{O}_{12}$  increases along with the increase in sintering temperature, while  $\text{TiO}_2$  phase decreases. This shows that the higher the sintering temperature, the more  $\text{Li}_4\text{Ti}_5\text{O}_{12}$  phase is formed. The persistence of impurity in the sample is due to the low holding time, Shenet al [12] managed to synthesize  $\text{Li}_4\text{Ti}_5\text{O}_{12}$  with pure phase at 800°C with sintering time of 4 hours, in addition, Wanget al [8] also managed to synthesize  $\text{Li}_4\text{Ti}_5\text{O}_{12}$  with high level of purity at a

temperature of 800°C for 15 hours. Therefore, impurity can be eliminated, one of which is by increasing the sintering time. The analysis results using the HIGHSCORE software on lattice parameters and lattice volume are shown in Table 2. The increase in temperature causes the lattice parameter values to increase and the lattice volume to enlarge. The lattice parameter values approach the lattice parameter values produced by Sun et al [14] ( $a = 8.35 \text{ \AA}$ ) and verde et al [15] ( $a = 8.351 \text{ \AA}$ ).

The results of morphological characterization of samples using SEM (Scanning Electron Microscope) with 10k and 1k SE enlargement can be seen in Figure 3. Morphologically, the surface of  $\text{Li}_4\text{Ti}_5\text{O}_{12}$  sample at a temperature of 500°C and 600°C has a rough texture, while a finer surface forms at 700°C, and at 800°C sample, the texture formed is finer than the other three samples. All samples consist of small and large particles that form agglomerations with particle shapes that are diverse such as round, rectangular, square and irregular shapes. But in the 800°C sample, grain boundaries began to form on large particles, so that smaller and finer particles of grain appeared. In this 800°C sample, there are also small particles that have a more regular shape and assemble to form one large material (bulk material).

**Table 2.** The lattice parameters of  $\text{Li}_4\text{Ti}_5\text{O}_{12}$  with variations of sintering temperatures using HIGHSCORE software..

Name of sampel	Lattice parameter (Å)	Lattice parameter (Å)
500°C	8.3344 (20)	578.93
600°C	8.3349 (7)	579.03
700°C	8.3568 (2)	583.61
800°C	8.3587 (1)	584

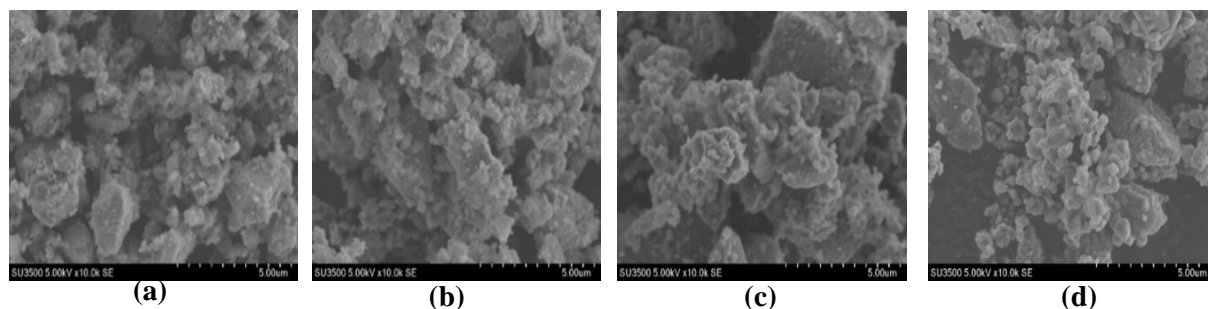


**Figure 3.** The morphology of  $\text{Li}_4\text{Ti}_5\text{O}_{12}$  samples as a result of characterization using SEM with enlargement of 10k SE with variations in sintering temperatures of (a) 500°C, (b) 600 °C, (c) 700 °C, (d) 800 °C.

In the Cyclic Voltammetry testing, half cell testing was conducted with a sample in the form of a coin cell. In this test,  $\text{Li}_4\text{Ti}_5\text{O}_{12}$  acting as a cathode was paired with lithium metal which acted as an anode as the voltage was lower than  $\text{Li}_4\text{Ti}_5\text{O}_{12}$ . Data from the Cyclic Voltammetry testing in the form of a curve that shows the relationship between voltage (V) as input and output in the form of current (I), the curve of the test results of Cyclic Voltammetry can be seen in Figure 4.

On the curve, there is a peak with an upward direction which shows the oxidation process called as anodic peak and a downward peak shows a reduction process as a cathodic peak. The reduction process occurs during the discharging, lithium ions move from the anode to the cathode while the oxidation process occurs when charging where the lithium ion moves in the opposite direction to the anode. The process of lithium moving from the anode to the cathode or alternatively is called

the intercalation and de-intercalation process of lithium ions. On Cyclic Voltammogram of  $\text{Li}_4\text{Ti}_5\text{O}_{12}$  at sintering temperatures of 500°C and 600°C shown by green and blue curves, both of them have oxidation peaks and other reductions, which are in the voltage range of 2.0 - 2.2 V and 1.5 - 1.75 V, the peak is the peak of reduction and oxidation of  $\text{TiO}_2$ . This is in accordance with the results of XRD characterization, that the material synthesized still contains considerable impurity.

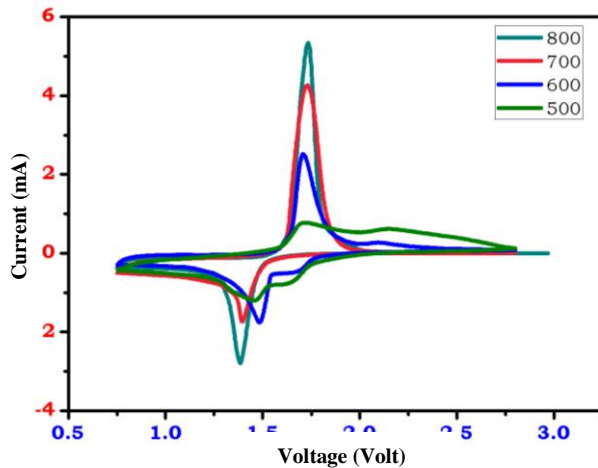


Figure 4.  $\text{Li}_4\text{Ti}_5\text{O}_{12}$  Cyclic voltammogram graph with variations of sintering temperatures.

From figure 4, it can be seen that the higher the sintering temperature, the higher the oxidation and reduction peaks, so the electric current produced is greater. High and sharp peaks indicate that the process of intercalation and de-intercalation of lithium ions is rapid. From the data of voltage and peak currents of the redox reaction, the magnitude of the diffusion coefficient of Li can be calculated using the Randles-Sevcik equation [16]:

$$i_p = 2.659 \times 10^5 n^3/2 A C D^{1/2} v^{1/2} \dots (1)$$

Where n is the number of electrons per molecule, A is the surface area ( $\text{cm}^2$ ), C is concentration of Li ion ( $\text{mol}/\text{cm}^3$ ), D is the diffusion coefficient of Li ion and v is the scan speed (V/s) and  $i_p$  is the peak current (A). The calculation results of the diffusion coefficient can be seen in table 3 as follows:

Table 3. The results of the calculation of the diffusion coefficient of  $\text{Li}_4\text{Ti}_5\text{O}_{12}$  with variations in sintering time.

Name of samples	$V_{\text{reduction}}$ (V)	$V_{\text{oxidation}}$ (V)	$V_{\text{polarization}}$ (V)	$I_p$ (mA)	D ( $\text{cm}^2/\text{S}$ )
500°C	1.4579	1.7076	0.2497	0.7721	$3.30 \times 10^{-11}$
600°C	1.4882	1.7103	0.2221	1.9341	$2.07 \times 10^{-10}$
700°C	1.3948	1.7268	0.3320	4.2537	$1.00 \times 10^{-9}$
800°C	1.3859	1.7348	0.3489	5.3444	$1.58 \times 10^{-9}$

From table 3, we can see that the difference in reduction and oxidation voltage (polarization voltage) of each sample increases with increasing sintering temperature, this polarization voltage shows the distance between the reduction and oxidation peak. In addition, the diffusion coefficient of Li ions also increases with

increasing sintering temperature. This indicates that the intercalation and de-intercalation of lithium ions takes place rapidly. In accordance with SEM results, particle size decreases along with increasing sintering temperature, the smaller particle size will result in easier ion transfer due to short diffusion length.

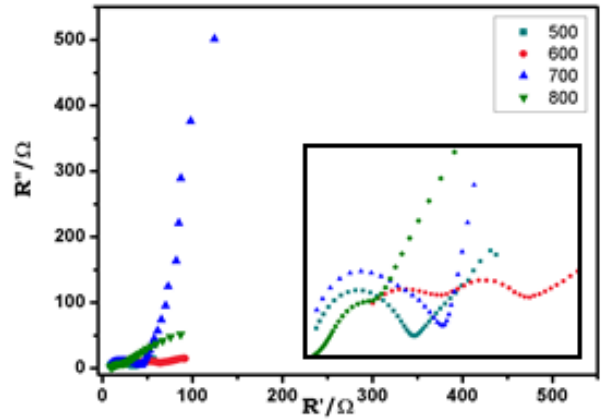


Figure 5.  $\text{Li}_4\text{Ti}_5\text{O}_{12}$  EIS graph with variations of sintering temperatures.

In EIS test results, the data obtained were then graphed in the form of a cole-cole plot as shown in Figure 5. All samples form semicircle arcs called "Nyquist Plots" and straight lines called impedances of Wargburg. From the graph, it can be seen that the resulting impedance has a real and imaginary component, the X axis represents the real impedance component (Z) and the Y axis as the imaginary impedance (Z') [17]. From the two impedances, the electronic resistance (Re) and charge transfer resistance (Rct) values can be calculated, where the values of both resistances will be used to calculate the conductivity value of  $\text{Li}_4\text{Ti}_5\text{O}_{12}$ .

In figure 5, the semicircular arc pattern that is formed decreases as the sintering temperature increases. In a semicircular arc pattern, the left side shows an electronic resistance value (Re), while the right side shows the charge transfer resistance (Rct) value. The electronic resistance value and charge transfer resistance value are the biggest in the 600°C sample. The straight line on the EIS curve shows the wargburg diffusion coefficient of Li ions. The more upright lines, the greater the value of the Li ion diffusion coefficient is. This means that Li ion intercalation and de-intercalation process takes place quickly. From figure 5, a sample of 700°C has a more upright line compared to the other samples. The conductivity value can be calculated using the following equation [16]:

$$\sigma = \rho \frac{l}{A} \dots (2)$$

Where R is the resistance ( $\Omega$ ), sample thickness is l (cm), sample surface area is A ( $\text{cm}^2$ ) and  $\rho$  is resistivity ( $\Omega \cdot \text{cm}$ ).

Data of conductivity calculation of  $\text{Li}_4\text{Ti}_5\text{O}_{12}$  can be seen in table 4 as follows:

**Table 4.** Conductivity calculation results of Li<sub>4</sub>Ti<sub>5</sub>O<sub>12</sub> with variations of sintering times.

Sampel	$\sigma_e$ (S/cm)	$\sigma_{ct}$ (S/cm)	$\sigma$ (S/cm)
500°C	0.0599	0.0164	0.0764
600°C	0.0291	0.0114	0.0406
700°C	0.0541	0.0118	0.0659
800°C	0.4621	0.1661	0.6282

From table 5 above, the highest conductivity was obtained in the sample with 800°C sintering temperature, whereas the lowest conductivity is shown by the sample with 600°C sintering temperature. So, the higher the sintering temperature, the greater the conductivity value is. During the sintering process, a crystallization process Li<sub>4</sub>Ti<sub>5</sub>O<sub>12</sub> occurred. At the sintering temperature of 500°C, the crystallization of Li<sub>4</sub>Ti<sub>5</sub>O<sub>12</sub> is not optimum and when the sample is sintered at 800°C the crystallization occurring has reached its maximum condition. When associated with the results of SEM characterization, at sintering temperature of 600°C, particle agglomeration occurs quite seriously so that the particle size of this sample is much larger. When the particle size is larger, the ion diffusion distance will be longer so that it will reduce the conductivity value.

Figure 6 shows the curve of charge-discharge testing of Li<sub>4</sub>Ti<sub>5</sub>O<sub>12</sub> with variations in sintering temperatures, the voltage applied between 1 - 2.5 Volt and current charge of 0.1C. In figure 6, Li<sub>4</sub>Ti<sub>5</sub>O<sub>12</sub> sample at a temperature of 500°C is shown by a green line, while LTO sample with a sintering temperature of 600°C is indicated by a red line. On both curves (500°C and 600°C), there is a step shape at the end of the curve, this indicates that the curve formed contains other phases other than Li<sub>4</sub>Ti<sub>5</sub>O<sub>12</sub> phase, this result confirms the XRD test results that the appearance of the steps is TiO<sub>2</sub>. In addition, the working voltage is in the range of 1.6 - 2.0 V.

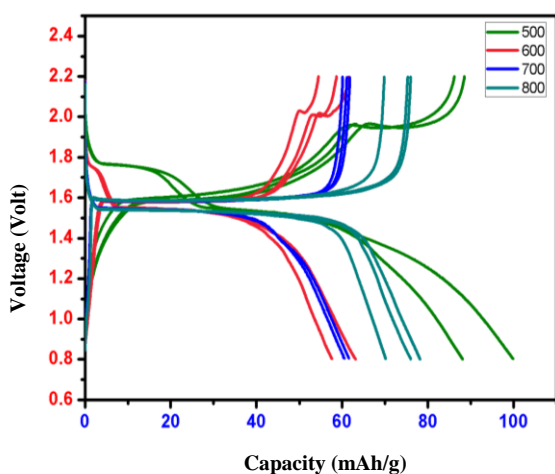


**Figure 7.** Charge-Discharge Graph of Li<sub>4</sub>Ti<sub>5</sub>O<sub>12</sub> with variations of sintering temperatures.

In the charge-discharge curve, the blue and greenish blue lines are Li<sub>4</sub>Ti<sub>5</sub>O<sub>12</sub> samples with sintering temperatures of 700°C and 800°C, on both curves, the voltage formed looks flat in the range of 1.55 V - 1.6 Volt (versus Li), this describes the main chemical reaction as a mechanism for transferring electron from a redox reaction, this curve does not detect impurity marked by no step shape at the end of the curve, but based on XRD results on all samples, there is impurity, except for LTO samples of 700°C and 800°C, the impurity content is only slight.

The charge-discharge analysis data of Li<sub>4</sub>Ti<sub>5</sub>O<sub>12</sub> with variations of sintering temperatures is shown in table 5. The highest capacity in the first cycle of charge-discharge is in the Li<sub>4</sub>Ti<sub>5</sub>O<sub>12</sub> sample with sintering temperature of 500°C as 88.45 mAh/g and 99.83 mAh/g. However, this large capacity is a combination of the capacities of Li<sub>4</sub>Ti<sub>5</sub>O<sub>12</sub> and TiO<sub>2</sub>. Even so, with the capacity produced at a temperature of 600°C is the total amount of capacity of Li<sub>4</sub>Ti<sub>5</sub>O<sub>12</sub> and TiO<sub>2</sub>. Battery capacity in samples with sintering temperature of 700°C is slightly higher than capacity in sample of 600°C which is 61.44 mAh/g and 63.08 mAh/g with a difference of 0.34 mAh/g, the battery capacity increases when the sintering temperature is increased to 800°C so the charge capacity obtained is 75.98 mAh/g and discharge as 78.07 mAh/g.

**Table 5.** Charge-discharge analysis data of Li<sub>4</sub>Ti<sub>5</sub>O<sub>12</sub> with variations of sintering temperatures.

Sample	Cycle	Capacity (mAh/g)	
		Charge	Discharge
500	1	88,45	99,83
	2	86,13	87,99
	3	83,55	-
600	1	61,49	63,08
	2	58,61	57,60
	3	54,44	-
700	1	61,75	61,63
	2	61,06	60,47
	3	60,10	-
800	1	75,98	78,07
	2	75,26	75,94
	3	69,80	70,07

From the table 7 we can also see that between the first and second and third cycles, the battery capacity produced at temperatures of 500°C and 600°C has decreased significantly with a difference of around ~ 2.3 - 2.5 mAh/g, while at sintering temperatures of 700°C and 800°C, the decrease in capacity is very small in the range of 0.6 - 0.96 mAh/g. This shows that TiO<sub>2</sub> Rutill is more stable compared to anatase TiO<sub>2</sub>. The capacity produced is still far from the battery capacity in a theoretical calculation that is equal to 175 mAh/g because the Li<sub>4</sub>Ti<sub>5</sub>O<sub>12</sub> material still contains the impurity of TiO<sub>2</sub>. This impurity decreases the conductivity value and the diffusion coefficient of the Lithium ion so that the resulting capacity is also still low. In addition, the thickness of the electrode is one of the factors that influence the battery storage capacity produced, in this study the electrodes made have a thickness of 0.03 mm.

Of course this thickness value is quite large, so that it can reduce the energy capacity produced, based on research conducted by Slamet et al. [18] that the thicker the electrode layer, the resistance value tends to increase, the conductivity value decreases because the thicker the layer increases electron mileage and the diffusion distance of lithium ions in the anode sheet is getting longer. The ability of energy storage capacity of lithium battery depends on the number of lithium ions stored in the electrode structure and how much can be moved during the charge and discharge process, because the number of electron currents stored and channeled is proportional to the number of lithium ions moving [19].

## CONCLUSION

The optimum temperature for sintering  $\text{Li}_4\text{Ti}_5\text{O}_{12}$  anode material with the sol gel method is  $800^\circ\text{C}$ . At this temperature, the impurity content of  $\text{TiO}_2$  is very small. The morphological structure produced is finer along with the increase in sintering temperature, but the particles are still agglomerated and the shape of the particles is not homogeneous. The resulting electrochemical performance has increased along with increasing sintering temperature, including voltammogram graphs, diffusion coefficient values, electrical conductivity and charge-discharge capacity. Of all the samples, the  $\text{Li}_4\text{Ti}_5\text{O}_{12}$  sintered at  $800^\circ\text{C}$  showed good electrochemical performance with a sharp and good voltammogram graph, the diffusion coefficient value of lithium ion was  $1,58 \times 10^{-9} \text{ cm}^2\text{s}^{-1}$ , electrical conductivity of  $0.6282 \text{ S/cm}$  and the discharge capacity given is  $78.07 \text{ mAh/g}$ .

## ACKNOWLEDGEMENT

Thank you to Kemenristekdikti for the Sinas program and Physics Research Center-LIPI for providing labs and testing facilities. We also thank the members of battery research for the discussion in helping to conduct the research and writing.

## REFERENCES

- [1]. P. G. Bruce, B. Scrosati, and J. Tarascon, "Lithium Batteries Nanomaterials for Rechargeable Lithium Batteries \*\* Angewandte," pp. 2930–2946, 2008.
- [2]. Y. Wang *et al.*, "Lithium and lithium ion batteries for applications in microelectronic devices: A review," *J. Power Sources*, vol. 286, pp. 330–345, 2015.
- [3]. Masaki Yoshio, Ralph J. Brodd, Akiya Kozawa, *Lithium-Ion Batteries*. New York: Springer, 2009.
- [4]. B. Zhao, R. Ran, M. Liu, and Z. Shao, "A comprehensive review of  $\text{Li}_4\text{Ti}_5\text{O}_{12}$  -based electrodes for lithium-ion batteries: The latest advancements and future perspectives," *Mater. Sci. Eng. R Reports*, vol. 98, pp. 1–71, 2015.
- [5]. X. Yang *et al.*, "Size-Tunable Single-Crystalline Anatase  $\text{TiO}_2$  Cubes as Anode Materials for Lithium Ion Batteries," *J. Phys. Chem. C*, vol. 119, no. 8, pp. 3923–3930, 2015.
- [6]. S. Zhang, X. Ge and C. Chen. "Synthesis of carbon-coated  $\text{Li}_4\text{Ti}_5\text{O}_{12}$  and its electrochemical performance as anode material for lithium-ion battery." *Chinese Chemical Letters*, vol.33, pp. 2274-2276, 2017
- [7]. Y. Kuo and J. Lin, "Electrochimica Acta One-pot sol-gel synthesis of  $\text{Li}_4\text{Ti}_5\text{O}_{12}/\text{C}$  anode materials for high-performance Li-ion batteries," *Electrochim. Acta*, vol. 142, pp. 43–50, 2014.
- [8]. R. P. Maloney, H. J. Kim, and J. S. Sakamoto, "Lithium titanate aerogel for advanced lithium-ion batteries," *ACS Appl. Mater. Interfaces*, vol. 4, no. 5, pp. 2318–2321, 2012.
- [9]. W. Yao, W. Zhuang, X. Ji, J. Chen, X. Lu, and C. Wang, "Solid-state synthesis of  $\text{Li}_4\text{Ti}_5\text{O}_{12}$  whiskers from  $\text{TiO}_2\text{-B}$ ." *Materials Research Bulletin*, vol. 75. pp. 204-210, 2016
- [10]. A. Mahmoud, J. M. Amarilla, and I. Saadoune, "Effect of thermal treatment used in the sol-gel synthesis of  $\text{Li}_4\text{Ti}_5\text{O}_{12}$  spinel on its electrochemical properties as anode for lithium ion batteries," *Electrochim. Acta*, vol. 163, pp. 213–222, 2015.
- [11]. C. Zhang, Y. Zhang, J. Wang, D. Wang, D. He, and Y. Xia, " $\text{Li}_4\text{Ti}_5\text{O}_{12}$  prepared by a modified citric acid sol gel method for lithium-ion battery," *J. Power Sources*, vol. 236, pp. 118–125, 2013.
- [12]. Y. C. Kuo, J. Y. Lin, "One-pot sol-gel synthesis of  $\text{Li}_4\text{Ti}_5\text{O}_{12}/\text{C}$  anode materials for high-performance Li-ion batteries." *Electrochim. Acta*, vol. 142, pp.43-50, 2014
- [13]. E. S. Endah yuniarti, Joko Triwibowo, "Pengaruh pH , Suhu dan Waktu pada Sintesis  $\text{LiFePO}_4/\text{C}$  dengan Metode Sol-Gel Sebagai Material Katoda untuk Baterai Sekunder Lithium," *Berk. MIPA*, vol. 23, no. 3, pp. 218–228, 2013.
- [14]. X. Sun, M. Hegde, Y. Zhang, M. He, L. Gu, Y. Wang, J. Shu, P. V. Radovanovic, and C. Cui, "Structure and Electrochemical Properties of Spinel  $\text{Li}_4\text{Ti}_5\text{O}_{12}$  Nanocomposites as Anode for Lithium-Ion Battery." *Int. J. Electrochem. Sci.*, vol. 9, pp. 1586-1596, 2014
- [15]. M. G. Verde, L. Baggetto, N. Balke, G. M. Veith, J. K. Seo, Z. Wang and Y. S. Meng, "Elucidating the Phase Transformation of  $\text{Li}_4\text{Ti}_5\text{O}_{12}$  Lithiation at the Nanoscale," *ACS Nano*, vol. 10, pp. 4312-4321. 2016
- [16]. J. Wang, *Analytical Electrochemistry*, Second., no. 1. New York: Wiley-VCH, 2014.
- [17]. K. Wu, J. Yang, X. Y. Qiu, J. M. Xu, Q. Q. Zhang, J. Jin and Q. C. Zhuang, "Study of spinel  $\text{Li}_4\text{Ti}_5\text{O}_{12}$  electrode reaction mechanism by electrochemical impedance spectroscopy." *Electrochim. Acta*, vol. 108, pp. 841-851. 2013

- [18]. Nordh, Tim. "Li<sub>4</sub>Ti<sub>5</sub>O<sub>12</sub> as an Anode material for Li Ion Batteries In Situ XRD and XPS Studies". Thesis, Uppsala Universitet. Feb.2013. electrochemical potentials of cathode materials in rechargeable batteries." *Material Today*, vol. 19, pp. 109-123, 2016
- [19]. C. Liu, Z. G. Neale, and G. Cao, "Understanding



Copyright © 2019 Jusami | Indonesian Journal of Materials Science. This article is an open access article distributed under the terms and conditions of the [Creative Commons Attribution-NonCommercial-ShareAlike 4.0 International License \(CC BY-NC-SA 4.0\)](https://creativecommons.org/licenses/by-nc-sa/4.0/).